

A ménage à trois of eV-scale sterile neutrinos, cosmology, and structure formation

Basudeb Dasgupta^{1,*} and Joachim Kopp^{2,†}

¹*International Centre for Theoretical Physics, Strada Costiera 11, 34014 Trieste, Italy.*

²*Max Planck Institut für Kernphysik, Saupfercheckweg 1, 69117 Heidelberg, Germany.*

(Dated: October 23, 2013)

We show that sterile neutrinos with masses $\gtrsim 1$ eV, as motivated by several short-baseline oscillation anomalies, can be consistent with cosmological constraints if they are charged under a hidden sector force mediated by a light boson. In this case, sterile neutrinos experience a large thermal potential that suppresses mixing between active and sterile neutrinos in the early Universe, even if vacuum mixing angles are large. Thus, the abundance of sterile neutrinos in the Universe remains very small, and their impact on Big Bang Nucleosynthesis, Cosmic Microwave Background, and large-scale structure formation is negligible. It is conceivable that the new gauge force also couples to dark matter, possibly ameliorating some of the small-scale structure problems associated with cold dark matter.

PACS numbers: 14.60.Pq, 98.80.-k, 95.35.+d

INTRODUCTION

Several anomalies in short baseline neutrino oscillation experiments have spurred interest in models with more than three neutrino species. In particular, the excesses of electron neutrino events in LSND [1] and Mini-BooNE [2], as well as the unexpected electron antineutrino disappearance at short baselines [3–6], could be explained in models with extra “sterile” neutrinos, i.e. light ($m \sim 1$ eV) new fermions that are uncharged under the Standard Model (SM) gauge group and mix with the three known neutrino species. On the other hand, a number of other neutrino oscillation experiments that did not observe any anomalous signals put such models under pressure [7–10], and a vigorous experimental program is currently underway to resolve the tension by either confirming the anomalies, or by providing a definitive null result.

It is often argued that the tightest constraints on sterile neutrino models come from cosmology. Indeed, the simplest models — with just one or several sterile neutrinos, but no other new particles — are disfavored by the Big Bang Nucleosynthesis (BBN) and Planck measurements of N_{eff} , the number of relativistic particle species in the early Universe [11, 12]. For sterile neutrino masses of ~ 1 eV, or larger, even tighter constraints are obtained from large-scale structure formation [13], where the presence of extra neutrino species would lead to a wash-out of structure due to efficient energy transport by neutrinos.

In this paper, we show that these constraints are evaded if sterile neutrinos have hidden interactions mediated, for instance, by a new gauge boson A' with a mass $M \lesssim \text{MeV}$. As discussed below, gauge forces of this type are also interesting in dark matter (DM) physics, and are probed in many cosmological and astrophysical searches [14]. We will show that at non-zero tem-

perature the sterile neutrinos feel a Mikheyev-Smirnov-Wolfenstein (MSW) potential that suppresses mixing between active and sterile neutrinos in the early Universe, thus preventing sterile neutrino production in the early Universe. We will discuss constraints on this scenario from cosmology and particle physics. In the last part of the paper we will also discuss the possibility that A' couples also to the DM in the Universe, possibly easing the disagreement between small-scale structure observations and cold DM simulations.

HIDDEN STERILE NEUTRINOS

We assume the Standard Model (SM) is augmented by one extra species of light ($\sim \text{eV}$) neutrinos ν_s , which do not couple to the SM gauge bosons but are charged under a new $U(1)_\chi$ gauge symmetry. We assume that ν_s have relatively large ($\sim 10\%$) vacuum mixing with the active neutrinos and is thus capable of explaining the short baseline oscillation anomalies.

The sterile sector is expected to be coupled to the SM sector through high-scale interactions, and the two sectors decouple at temperatures $\gtrsim \text{TeV}$. Our results remain qualitatively correct even for decoupling temperatures as low as 1 GeV, i.e., just above the QCD phase transition. After decoupling, the temperature T_s of the sterile sector continues to drop as $T_s \sim 1/a$ (a being the scale factor of the Universe), while the temperature in the visible sector, T_γ , drops more slowly because of the entropy generated when heavier degrees of freedom (unstable hadrons, positrons, etc.) become inaccessible and annihilate or decay away. By the BBN epoch, the number of effective degrees of freedom of the visible sector, g_* , decreases from $\simeq 106.7$ to $\simeq 10.75$. Taking the sterile sector temperature as $T_s = (g_{*,\text{TeV}}/g_{*,T_\gamma})^{1/3} T_\gamma$, the ad-

ditional effective number of fully-thermalized neutrinos at BBN, for a single left-handed sterile neutrino (and its right-handed antineutrino) and a relativistic A' , is

$$\Delta N_\nu \equiv \frac{\rho_{\nu_s} + \rho_{A'}}{\rho_\nu} = \frac{(g_{\nu_s} + g_{A'}) T_s^4}{g_\nu T_\nu^4} \quad (1)$$

$$= \frac{(\frac{7}{8} \times 2 + 3) \times (\frac{10.75}{106.75})^{\frac{4}{3}}}{(\frac{7}{8} \times 2) \times (\frac{4}{11})^{\frac{4}{3}}} \simeq 0.5, \quad (2)$$

which is easily consistent with the bound from BBN, viz., $\Delta N_\nu = 0.66_{-0.45}^{+0.47}$ [11]. Up to 3 generations of sterile neutrinos could be accommodated within $\simeq 1\sigma$. Note that we have conservatively taken T_ν at the end of BBN.

At lower temperatures, $T_s \lesssim 0.1 \text{ MeV}$, A' becomes nonrelativistic, and decays to sterile neutrinos, heating them up by a factor of $\simeq 1.4$. However, these neutrinos with masses $m \gtrsim 1 \text{ eV}$, are nonrelativistic by the epoch of matter-radiation equality ($T_\gamma \simeq 0.7 \text{ eV}$) and recombination ($T_\gamma \simeq 0.3 \text{ eV}$). Thus the impact of thermal abundances of A' and ν_s on the CMB and structure formation is negligible. See also [15–17] for alternate approaches. We will now show that oscillations of active neutrinos into sterile neutrinos, which are normally expected to bring the two sectors into equilibrium again, are also strongly suppressed due to “matter” effects.

The basic idea underlying our proposal is similar to the high-temperature counterpart of the MSW effect. Let us recall that at high temperatures, i.e., in the early Universe, a neutrino with energy E experiences a potential $V_{\text{MSW}} \propto G_F^2 E T_\gamma^4$ due to their own *energy density* [18]. This is not zero even in a CP symmetric Universe.

A similar, but much larger, potential can be generated at high-temperature for sterile neutrinos, if they couple to a light hidden gauge boson A' . There are two types of processes that can contribute to this potential — the sterile neutrino can forward-scatter off an A' in the medium (left diagram in Fig. 1), or off a fermion f that couples to A' (right diagram in Fig. 1).

These interactions of the sterile neutrino with the medium modify its dispersion relation through a potential V_{eff} :

$$E = |\mathbf{k}| + \frac{m^2}{2E} + V_{\text{eff}}, \quad (3)$$

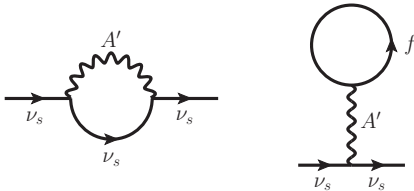


Figure 1. Bubble and tadpole contributions to the sterile neutrino self-energy, which create an effective “matter” potential.

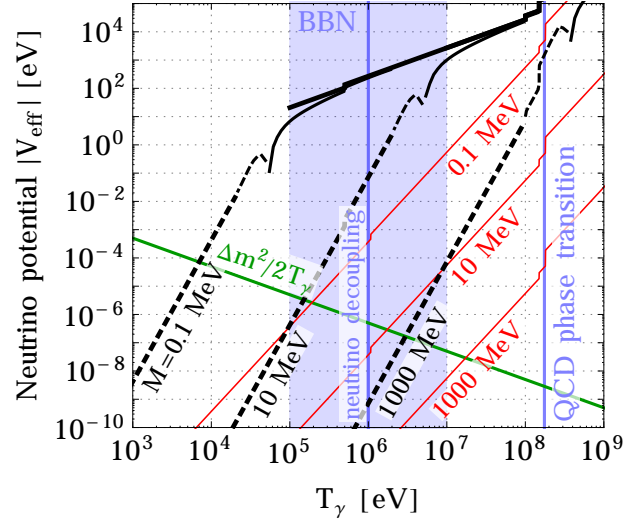


Figure 2. Matter potential for sterile neutrinos of energy $E \sim T_\gamma$ as a function of the photon temperature T_γ , for a hidden sector fine-structure constant $\alpha_\chi \equiv e_\chi^2/(4\pi) = 10^{-2}/(4\pi)$. Black curves show $|V_{\text{eff}}|$ for different values of the gauge boson mass M , with solid lines corresponding to $V_{\text{eff}} > 0$ and dashed lines indicating $V_{\text{eff}} < 0$. Thin (Thick) lines show exact numerical (approximate analytical) results. The green line is the vacuum neutrino oscillation frequency between active and sterile flavors for $\Delta m^2 = 1 \text{ eV}^2$. As long as $\Delta m^2/(2T_\gamma) \ll |V_{\text{eff}}|$, oscillations are suppressed. The QCD phase transition and active neutrino decoupling epochs are annotated. Red lines show the contribution to V_{eff} from an asymmetric DM particle with $m_\chi = 1 \text{ GeV}$. The small kinks in the curves are due to changes in g_* , the effective number of degrees of freedom in the Universe.

where E and $|\mathbf{k}|$ are the energy and momentum of the sterile neutrino.

We calculated V_{eff} using the real time formalism in thermal field theory (see Appendix A). Physically, this potential is the correction to the sterile neutrino self-energy. In the low-temperature limit, i.e., $T_s, E \ll M$,

$$V_{\text{eff}} \simeq -\frac{28\pi^3 \alpha_\chi E T_s^4}{45 M^4}, \quad (4)$$

similar to the potential for active neutrinos [18], with $\alpha_\chi \equiv e_\chi^2/(4\pi)$ being the $U(1)_\chi$ fine-structure constant. In the high-temperature limit, $T_s, E \gg M$, the potential is

$$V_{\text{eff}} \simeq \frac{\pi \alpha_\chi T_s^2}{2E}, \quad (5)$$

similar to the result for hot QED [19]. We have assumed that there is no asymmetry in ν_s , which may be interesting to consider [15, 20].

These analytical results are plotted in Fig. 2 (thick black lines). For comparison, we also calculated the potential numerically (thin black lines), and found excellent consistency with the analytical approximations in their region of validity. The potential is small only in a very

small range of temperatures $T_s \approx M$, where the potential changes sign and goes through zero. Note that the potential is always smaller than $|\mathbf{k}|$ and vanishes at zero temperature.

In the presence of a potential, it is well-known that neutrino mixing angles are modified. In the two-flavor approximation, the effective mixing angle θ_m in matter is given by [21]

$$\sin^2 2\theta_m = \frac{\sin^2 2\theta_0}{\left(\cos 2\theta_0 + \frac{2E}{\Delta m^2} V_{\text{eff}}\right)^2 + \sin^2 2\theta_0}, \quad (6)$$

where θ_0 is the vacuum mixing angle, and $\Delta m^2 = m_s^2 - m_a^2$ is the difference between the squares of the mostly sterile mass eigenstate m_s and the active neutrino mass scale m_a . If the potential is much larger than the vacuum oscillation frequency, i.e.,

$$|V_{\text{eff}}| \gg \left| \frac{\Delta m^2}{2E} \right|, \quad (7)$$

then θ_m will be tiny, and oscillations of active neutrinos into sterile ones are suppressed.

This is confirmed by Fig. 2, which summarizes our main results. For a typical neutrino energy $E \sim T_\gamma$ and $M \lesssim 10$ MeV, we see that condition (7) is well-satisfied down to temperatures $T_\gamma \lesssim 1$ MeV, i.e., until after the time of neutrino decoupling, when their thermal production becomes impossible. Thus θ_m is suppressed and sterile neutrinos are not produced in significant numbers. Oscillations after decoupling reduces a small fraction, $\sin^2 2\theta_m \lesssim 0.1$, of the active neutrinos to steriles (which are nonrelativistic below 1 eV), consistent with $N_{\text{eff}} = 3.30^{+0.54}_{-0.51}$ from Planck data [12]. Note that in Fig. 2, we have conservatively taken sterile neutrino decoupling to occur at the same temperature, $T_\gamma \simeq 1$ MeV, as the decoupling of active neutrinos. In reality, sterile neutrino production ceases when $\Gamma_s \sim \sin^2 \theta_s G_F^2 T_\gamma^5$ drops below the Hubble expansion rate $H \propto T_\gamma^2$, which happened at temperatures around $1 \text{ MeV}/(\sin^2 \theta)^{1/3}$.

Even for M slightly larger than 1 MeV, sterile neutrino production remains suppressed until the BBN epoch, but it is interesting that in this case V_{eff} crosses zero while neutrinos are still in thermal equilibrium. This implies that there is a brief time-period during which sterile neutrinos could be produced efficiently. However, as long as its duration is much shorter than inverse of the sterile neutrino production rate $\Gamma_s^{-1} \sim [\sin^2 \theta_s G_F^2 T_\gamma^5]^{-1}$, only partial thermalization of sterile neutrinos will occur. Interestingly, at the MSW resonance, i.e., $\Delta m^2 \simeq -2EV_{\text{eff}}$, one may get some active-to-sterile neutrino (or antineutrino) conversion, depending on the adiabaticity of this resonance. This implies that, for $M \gtrsim 10$ MeV, we predict a fractional value of ΔN_{eff} at BBN. A study of the detailed dynamics during this epoch is beyond the scope of our present work.

As a final remark, we would like to emphasize that, while Fig. 2 is for $E = T_\gamma$, it is important to keep in mind that active neutrinos follow a thermal distribution. We have checked that even for E different from T_γ , the value of V_{eff} does not change too much. Therefore, our conclusions regarding the suppression of sterile neutrino production remain valid even when the tails of the thermal distribution are taken into account.

COUPLING TO DARK MATTER

If a new gauge force of the proposed form exists, it is conceivable that not only sterile neutrinos, but also DM particles couple to it. This of course leads to an additional contribution $2\pi\alpha_\chi(n_\chi - n_{\bar{\chi}})/M^2$ to V_{eff} (see Appendix A), through the tadpole diagram in Fig. 1. As long as DM is CP-symmetric, we have $n_\chi - n_{\bar{\chi}} = 0$ and this extra contribution vanishes. Even for asymmetric DM [22], we see in Fig. 2 (red lines) that it is usually subleading for $m_\chi \gtrsim 1$ GeV.

The extra gauge interaction of DM does, however, lead to DM self-scattering, which has received considerable attention recently as a way of solving [23–25] the existing disagreement between the observed substructure of DM in the Milky Way and N-body simulations of galaxy formation. In particular, self-interacting DM can solve the “too big to fail” problem [26, 27], i.e., the question why very massive DM subhaloes that are predicted to exist in a Milky Way type galaxy have not been observed, even though one would expect star formation to be efficient in them and make them appear as luminous dwarf galaxies. Similarly, DM self-interactions could be the reason why the Milky Way appears to have fewer dwarf galaxies than expected from simulations (the “missing satellites” problem [28]). Finally, it may be possible to explain why the observed DM density distribution in Milky Way subhaloes appears to exhibit a constant density core [29, 30] rather than a steep cusp predicted in N-body simulations [31] (“cusp vs. core problem”). While all these problems could well have different explanations — for instance the impact of baryonic feedback on N-body simulations is not yet well understood — it is intriguing that the self-scattering cross sections predicted in the scenario discussed here has exactly the right properties to mitigate these small-scale structure issues.

In our model, the “energy transfer cross section” in the center of mass frame, $\sigma_T = \int d\Omega d\sigma/d\Omega(1 - \cos \theta)$, is given at tree-level by [32]

$$\sigma_T \simeq \frac{8\pi\alpha_\chi^2}{m_\chi^2 v_{\text{rel}}^4} \left[\log(1 + R^2) - \frac{R^2}{1 + R^2} \right], \quad (8)$$

with $R \equiv m_\chi v_{\text{rel}}/M$. Here, v_{rel} is the relative velocity of the two colliding DM particles. It is easy to see that σ_T is velocity independent for $v_{\text{rel}} \ll M/m_\chi$ and drops

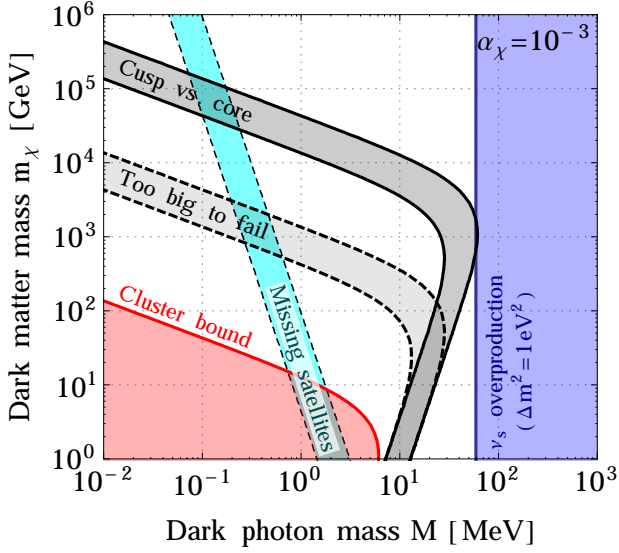


Figure 3. Constraints on DM self-interactions from the requirements that the self-interaction in galaxy clusters is small, i.e., $\langle\sigma_T\rangle/m_\chi \lesssim 1 \text{ cm}^2/\text{g}$, and that production of 1 eV sterile neutrinos is suppressed, i.e., $\sin^2 2\theta_m \lesssim 10^{-3}$ at $T_\gamma = 1 \text{ MeV}$. We also show the favored parameter region for mitigating the cusp vs. core and too big to fail problems, i.e., $\langle\sigma_T\rangle/m_\chi = 0.1 - 1 \text{ cm}^2/\text{g}$ in dwarf and Milky Way sized galaxies, respectively, and solving the missing satellites problem ($M_{\text{cut}} = 10^9 - 10^{10} M_{\text{Sun}}$).

roughly $\propto v_{\text{rel}}^{-4}$ for larger $v_{\text{rel}} \gg M/m_\chi$. This implies that the velocity-averaged cross section per unit DM mass, $\langle\sigma_T\rangle/m_\chi$, can be of order $0.1 - 1 \text{ cm}^2/\text{g}$ in galaxies ($v_{\text{rel}} \sim \mathcal{O}(100 \text{ km/sec})$), as required to mitigate the small-scale structure problems [24, 25], while remaining well below this value in galaxy clusters ($v_{\text{rel}} \sim \mathcal{O}(1000 \text{ km/sec})$), from which the most robust constraints are obtained [33]. In computing $\langle\sigma_T\rangle$, we assume the DM velocity distribution to be of Maxwell-Boltzmann form, with velocity dispersion v_{rel} .

As for the missing satellites problem, it was shown in [34–36] that DM–neutrino scattering can delay kinetic decoupling of DM and increase the cut-off in the structure power spectrum to the scales of the dwarf galaxies. Quantitatively [35],

$$\frac{M_{\text{cut}}}{M_{\text{Sun}}} \simeq 3.2 \times 10^{13} \alpha_\chi^{\frac{3}{2}} \left(\frac{T_s}{T_\gamma}\right)_{\text{kd}}^{\frac{3}{2}} \left(\frac{\text{TeV}}{m_\chi}\right)^{\frac{3}{4}} \left(\frac{\text{MeV}}{M}\right)^3. \quad (9)$$

Thus, the cut-off can be raised to $M_{\text{cut}} = 10^9 - 10^{10} M_{\text{Sun}}$, as required to solve the missing satellites problem [35]. The number of sterile neutrino generations N_s , assumed to be 1 here, only weakly impacts the result as $M_{\text{cut}} \propto N_s^{-3/4}$. Note that in contrast to Ref. [35], we obtain a small T_s/T_γ , from decays of heavy Standard Model particles after the decoupling of the sterile sector.

In Fig. 3, we show the region of parameter space favored by these considerations. We see that for $M = 0.1 - 10 \text{ MeV}$, DM masses $m_\chi = 1 - 100 \text{ TeV}$, and $\alpha_\chi = 10^{-3}$ (see Appendix B for dependence on α_χ), it is possible to mitigate the cusp vs. core and/or too big to fail problems, as well as the missing satellites problem, while remaining consistent with the cluster constraint and simultaneously suppressing sterile neutrino production to evade BBN and CMB constraints. This potentially interesting solution to enduring problems with small-scale structures was first shown in a scenario with active neutrinos [35], which has since been constrained using laboratory data, BBN, and large-scale structure [37–39], and a qualitative extension to sterile neutrinos was suggested therein.

The DM relic abundance may be produced by Sommerfeld-enhanced annihilations of DM into A' pairs that decay to sterile neutrinos. However, unlike in [35], we do not use separate couplings of DM and ν to do this, so this should identify the preferred value for DM mass in the range $m_\chi \sim 1 - 100 \text{ TeV}$. As long as DM chemical freeze-out happens well above $T_\gamma \sim \text{GeV}$ and the sterile neutrinos have time to rethermalize with ordinary neutrinos (and photons) via high-scale interactions, our scenario remains unaltered by DM annihilation.

DISCUSSION AND SUMMARY

We now discuss the possible origin of a new gauge force in the sterile neutrino sector, and on further phenomenological consequences. In [40], Pospelov has proposed a model with sterile neutrinos charged under gauged baryon number. He has argued that the model is consistent with low energy constraints, in particular the one from $K \rightarrow \pi\pi\nu\nu$, even for $\kappa^2 \sin \theta/M^2 \sim 1000 G_F$. This is precisely the parameter region in which sterile neutrino production in the early Universe is suppressed, as we have demonstrated above. In [40–42], the phenomenological consequences of this model have been investigated, and it has been shown that strong anomalous scattering of solar neutrinos in DM detectors is expected. As an alternative to gauged baryon number, sterile neutrinos could also be charged under a gauge force that mixes kinetically with the photon [41]. In this case, $M \gtrsim 10 \text{ MeV}$ is preferred unless the coupling constants are extremely tiny. Once again in this model interesting solar neutrino signals in DM detectors can occur. Finally, while we have focused here on new gauge interactions, it is also conceivable that the new interaction is instead mediated by a scalar. We do not expect our conclusions to change qualitatively in this case.

In summary, we have shown that eV-scale sterile neutrinos can be consistent with cosmological data from BBN, CMB, and large-scale structure if we allow them to be charged under a new gauge interaction mediated by a MeV-scale boson. In this case, sterile neutrino pro-

duction in the early Universe is suppressed due to the thermal MSW potential generated by the mediator and by sterile neutrinos themselves. Our proposed scenario leads to a small fractional number of extra relativistic degrees of freedom in the early Universe, which may be experimentally testable in the future. If the considered boson also couples to DM, it could simultaneously explain observed departures of small-scale structures from the predictions of cold DM simulations.

ACKNOWLEDGMENTS

We are grateful to Xiaoyong Chu and Georg Raffelt for useful discussions. JK would like to thank the Aspen Center for Physics, funded by the US National Science Foundation under grant No. 1066293, for kind hospitality and support during part of this work. We acknowledge the use of the FeynCalc [43] and JaxoDraw [44] packages. Ref. [45] appeared the day we submitted our paper to arXiv, and addresses active-sterile oscillations in the presence of a hidden force mediated by a slightly more massive mediator ($M \gtrsim 100$ MeV).

Appendix A

Here, we derive the dispersion relation for sterile neutrinos coupled to a $U(1)_\chi$ gauge force in the regime of nonzero temperature and density. Our approach closely follows [18, 19, 46, 47].

From considerations of Lorentz invariance, the sterile neutrino self energy at one-loop can be expressed as

$$\Sigma(k) = (m - a\not{k} - b\not{u})P_L. \quad (10)$$

Here, $P_L = (1 - \gamma^5)/2$ is a chirality projector, m is the sterile neutrino mass, p is its 4-momentum and u is the 4-momentum of the heat bath. We work in the rest frame of the heat bath, so we take $u = (1, 0, 0, 0)$.

This thermal self-energy modifies the dispersion relation to

$$\det(\not{k} - \Sigma(k)) = 0, \quad (11)$$

which, in the ultrarelativistic regime, $k^0 \approx |\mathbf{k}|$, gives

$$k^0 = |\mathbf{k}| + \frac{m^2}{2|\mathbf{k}|} - b \quad (12)$$

to linear order in the coefficients a and b . Note that the usual dispersion relation for an ultrarelativistic neutrino, $k^0 = |\mathbf{k}| + \frac{m^2}{2|\mathbf{k}|}$, is modified by an effective potential

$$V_{\text{eff}} \equiv -b. \quad (13)$$

The coefficient b can then be obtained according to the relation

$$b = \frac{1}{2\mathbf{k}^2} [(k^0)^2 - \mathbf{k}^2] \text{tr} \not{u} \Sigma(k) - k^0 \text{tr} \not{k} \Sigma(k). \quad (14)$$

So, the remaining job is to calculate $\Sigma(k)$.

We assume a Lagrangian $\mathcal{L}_{\text{int}} = e_\chi \bar{f} \gamma^\mu P_L f A'_\mu$, where e_χ is the $U(1)_\chi$ gauge coupling. At lowest order, $\Sigma(k)$ receives contributions from the bubble and tadpole diagrams shown in Fig. 1. In the real time formalism, these diagrams are calculated using the unitary gauge thermal propagators for the fermion,

$$S(p) = (\not{p} + m) \left[\frac{1}{p^2 - m^2} + i\Gamma_f(p) \right], \quad (15)$$

and the gauge boson

$$D^{\mu\nu}(p) = (-g^{\mu\nu} + p^\mu p^\nu / M^2) \left[\frac{1}{p^2 - M^2} + i\Gamma_b(p) \right]. \quad (16)$$

The thermal parts are given by

$$\Gamma_f(p) = 2\pi\delta(p^2 - m^2)\eta_f(p), \quad (17)$$

$$\Gamma_b(p) = 2\pi\delta(p^2 - M^2)\eta_b(p), \quad (18)$$

respectively, with the distribution functions

$$\eta_f(p) = [e^{|p \cdot u|/T_s} + 1]^{-1}, \quad (19)$$

$$\eta_b(p) = [e^{|p \cdot u|/T_s} - 1]^{-1}. \quad (20)$$

The form of $S(p)$ and $D^{\mu\nu}(p)$ can be understood from the fact that at finite temperature and density, there are not only virtual ν_s and A' in the medium, but also real particles that have been thermally excited.

The diagrams in Fig. 1 are given by

$$\Sigma_{\text{bubble}}(k) = -ie_\chi^2 \int \frac{d^4 p}{(2\pi)^4} \gamma^\mu P_L iS(p+k) \gamma^\nu iD_{\mu\nu}(p), \quad (21)$$

$$\Sigma_{\text{tadpole}}(k) = ie_\chi^2 \gamma^\mu P_L iD_{\mu\nu}(0) \int \frac{d^4 p}{(2\pi)^4} \text{tr} \left[\gamma^\nu P_L iS(p) \right]. \quad (22)$$

Since we are interested in the leading thermal corrections, we evaluate only terms proportional to one power of Γ_f or Γ_b .

The leading thermal contributions to the bubble diagram are

$$e_\chi^2 \int \frac{d^4 p}{(2\pi)^4} \gamma^\mu (\not{k} + \not{p}) \gamma^\nu P_L \left(-g_{\mu\nu} + \frac{p_\mu p_\nu}{M^2} \right) \times \left[\frac{i\Gamma_f(k+p)}{p^2 - M^2} - \frac{i\Gamma_b(p)}{(k+p)^2 - m^2} \right]. \quad (23)$$

We evaluate this expression by first using the δ -functions in Γ_f and Γ_b to carry out the p^0 integral. The remaining 3-momentum integral can be evaluated in spherical coordinates, with the z -axis defined by the direction of \mathbf{k} . In this coordinate system, the integral over the azimuthal angle is trivial, and the second angular integral can be evaluated. We have checked that at this stage our results agree with those of [47] if we neglect the contributions of longitudinal polarization state of the gauge boson, as these authors have done.

The remaining integral over $|\mathbf{p}|$ can be carried out numerically, but we derive analytical approximations for the two important limiting cases. In the limit of small temperatures, $|\mathbf{k}|, T_s \ll M$, we expand to leading order in $|\mathbf{p}|/M$, and obtain

$$b = \frac{7e_\chi^2 |\mathbf{k}|}{6\pi^2 M^4} \int_0^\infty d|\mathbf{p}| |\mathbf{p}|^3 (\eta_f + \eta_{\bar{f}}) \quad (24)$$

$$= \frac{7e_\chi^2 |\mathbf{k}| \pi^2 T_s^4}{45M^4}. \quad (25)$$

In the opposite limit of high temperature, $|\mathbf{k}|, T_s \gg M$, we can drop subleading logarithmic terms in $|\mathbf{p}|$, and the linear term gives

$$b = -\frac{e_\chi^2}{4\pi^2 |\mathbf{k}|} \int_0^\infty d|\mathbf{p}| |\mathbf{p}| (\eta_f + \eta_{\bar{f}} + 2\eta_b) \quad (26)$$

$$= -\frac{e_\chi^2 T_s^2}{8|\mathbf{k}|}. \quad (27)$$

Note that the potential $|b| \ll |\mathbf{k}|$, thus the neutrinos are still ultrarelativistic, and we can replace $|\mathbf{k}| \approx k^0 = E$, inside the potential.

In terms of the $U(1)_\chi$ fine-structure constant, $\alpha_\chi \equiv e_\chi^2/(4\pi)$, we thus arrive at,

$$V_{\text{eff}}^{\text{bubble}} \simeq \begin{cases} -\frac{28\pi^3 \alpha_\chi E T_s^4}{45M^4} & \text{for } T_s, E \ll M \\ +\frac{\pi \alpha_\chi T_s^2}{2E} & \text{for } T_s, E \gg M \end{cases} \quad (28)$$

which is the result used in the main text.

Similarly, calculating the tadpole diagram gives

$$V_{\text{eff}}^{\text{tadpole}} \simeq \frac{2\pi \alpha_\chi}{M^2} (n_f - n_{\bar{f}}), \quad (29)$$

in terms of terms of the number density of background fermions. It is straightforward to see that $\Sigma_{\text{tadpole}}(k)$ vanishes when there is no fermion asymmetry. In this work, we have assumed that ν_s does not have an asymmetry, but instead consider the possibility that A' couples to asymmetric DM χ , with a net number density, $n_\chi - n_{\bar{\chi}}$, which can provide this potential.

Appendix B

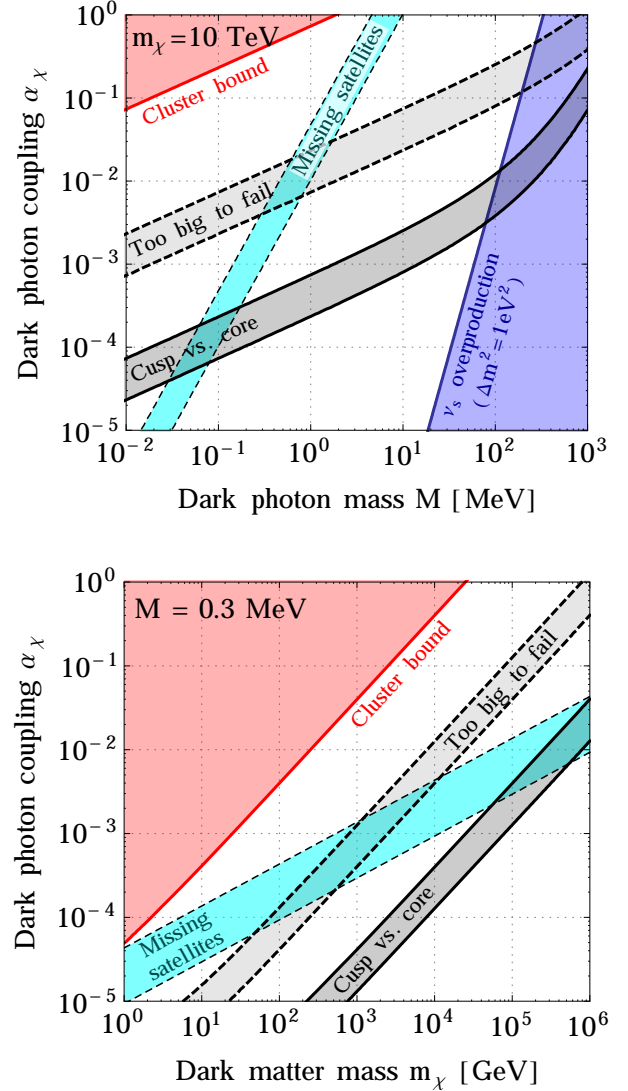


Figure 4. In analogy to Fig. 3, these plots show the dependence of DM self-scattering constraints on the DM coupling for a fixed DM mass $m_\chi = 10$ TeV (top panel) and fixed gauge boson mass $M = 0.3$ MeV (bottom panel).

In Fig. 4 we show that the DM results, shown in the main text, are valid over a reasonable range of values for the coupling α_χ . We find that the favorable value for the coupling increases with larger m_χ . The mediator boson mass remains in the MeV range. Note that, in the bottom panel of Fig. 4, the neutrino oscillation constraints are below the range of the figure.

* bdasgupta@ictp.it

† jkopp@mpi-hd.mpg.de

- [1] A. Aguilar et al. (LSND), Phys. Rev. **D64**, 112007 (2001), hep-ex/0104049.
- [2] A. Aguilar-Arevalo et al. (MiniBooNE Collaboration) (2012), 1207.4809.
- [3] T. Mueller, D. Lhuillier, M. Fallot, A. Letourneau, S. Cormon, et al., Phys.Rev. **C83**, 054615 (2011), 1101.2663.
- [4] G. Mention, M. Fechner, T. Lasserre, T. Mueller, D. Lhuillier, et al., Phys.Rev. **D83**, 073006 (2011), 1101.2755.
- [5] A. Hayes, J. Friar, G. Garvey, and G. Jonkmans (2013), 1309.4146.
- [6] M. A. Acero, C. Giunti, and M. Laveder, Phys.Rev. **D78**, 073009 (2008), 0711.4222.
- [7] J. Kopp, M. Maltoni, and T. Schwetz, Phys.Rev.Lett. **107**, 091801 (2011), 1103.4570.
- [8] J. Kopp, P. A. N. Machado, M. Maltoni, and T. Schwetz (2013), 1303.3011.
- [9] J. Conrad, C. Ignarra, G. Karagiorgi, M. Shaevitz, and J. Spitz (2012), 1207.4765.
- [10] J. R. Kristiansen, O. y. Elgarø y, C. Giunti, and M. Laveder (2013), 1303.4654.
- [11] G. Steigman, Adv.High Energy Phys. **2012**, 268321 (2012), 1208.0032.
- [12] P. Ade et al. (Planck Collaboration) (2013), 1303.5076.
- [13] J. Hamann, S. Hannestad, G. G. Raffelt, and Y. Y. Wong, JCAP **1109**, 034 (2011), 1108.4136.
- [14] J. Jaeckel and A. Ringwald, Ann.Rev.Nucl.Part.Sci. **60**, 405 (2010), 1002.0329.
- [15] R. Foot and R. Volkas, Phys.Rev.Lett. **75**, 4350 (1995), hep-ph/9508275.
- [16] V. Barger, J. P. Kneller, P. Langacker, D. Marfatia, and G. Steigman, Phys.Lett. **B569**, 123 (2003), hep-ph/0306061.
- [17] C. M. Ho and R. J. Scherrer (2012), 1212.1689.
- [18] D. Nötzold and G. Raffelt, Nucl.Phys. **B307**, 924 (1988).
- [19] H. A. Weldon, Phys.Rev. **D26**, 2789 (1982).
- [20] N. Saviano, A. Mirizzi, O. Pisanti, P. D. Serpico, G. Mangano, et al. (2013), 1302.1200.
- [21] E. K. Akhmedov (1999), hep-ph/0001264.
- [22] K. M. Zurek (2013), 1308.0338.
- [23] M. Vogelsberger, J. Zavala, and A. Loeb, Mon.Not.Roy.Astron.Soc. **423**, 3740 (2012), 1201.5892.
- [24] M. Rocha, A. H. Peter, J. S. Bullock, M. Kaplinghat, S. Garrison-Kimmel, et al., Mon.Not.Roy.Astron.Soc. **430**, 81 (2013), 1208.3025.
- [25] J. Zavala, M. Vogelsberger, and M. G. Walker (2012), 1211.6426.
- [26] M. Boylan-Kolchin, J. S. Bullock, and M. Kaplinghat, Mon.Not.Roy.Astron.Soc. **415**, L40 (2011), 1103.0007.
- [27] M. Boylan-Kolchin, J. S. Bullock, and M. Kaplinghat, Mon.Not.Roy.Astron.Soc. **422**, 1203 (2012), 1111.2048.
- [28] A. A. Klypin, A. V. Kravtsov, O. Valenzuela, and F. Prada, Astrophys.J. **522**, 82 (1999), astro-ph/9901240.
- [29] B. Moore, Nature **370**, 629 (1994).
- [30] R. A. Flores and J. R. Primack, Astrophys.J. **427**, L1 (1994), astro-ph/9402004.
- [31] J. F. Navarro, C. S. Frenk, and S. D. M. White, Astrophys. J. **490**, 493 (1997), astro-ph/9611107.
- [32] J. L. Feng, M. Kaplinghat, and H.-B. Yu, Phys.Rev.Lett. **104**, 151301 (2010), 0911.0422.
- [33] P. J. Fox and M. R. Buckley (2009), 0911.3898.
- [34] T. Bringmann and S. Hofmann, JCAP **0407**, 016 (2007), hep-ph/0612238.
- [35] L. G. van den Aarssen, T. Bringmann, and C. Pfrommer, Phys.Rev.Lett. **109**, 231301 (2012), 1205.5809.
- [36] I. M. Shoemaker (2013), 1305.1936.
- [37] R. Laha, B. Dasgupta, and J. F. Beacom (2013), 1304.3460.
- [38] B. Ahlgren, T. Ohlsson, and S. Zhou (2013), 1309.0991.
- [39] F.-Y. Cyr-Racine, R. de Putter, A. Raccanelli, and K. Sigurdson (2013), 1310.3278.
- [40] M. Pospelov, Phys.Rev. **D84**, 085008 (2011), 1103.3261.
- [41] R. Harnik, J. Kopp, and P. A. Machado, JCAP **1207**, 026 (2012), 1202.6073.
- [42] M. Pospelov and J. Pradler, Phys.Rev. **D85**, 113016 (2012), 1203.0545.
- [43] R. Mertig, M. Bohm, and A. Denner, Comput. Phys. Commun. **64**, 345 (1991).
- [44] D. Binosi, J. Collins, C. Kaufhold, and L. Theussl, Comput.Phys.Comm. **180**, 1709 (2009), 0811.4113.
- [45] S. Hannestad, R. S. Hansen, and T. Tram (2013), 1310.5926.
- [46] K. Enqvist, K. Kainulainen, and J. Maalampi, Nucl.Phys. **B349**, 754 (1991).
- [47] C. Quimbay and S. Vargas-Castrillon, Nucl.Phys. **B451**, 265 (1995), hep-ph/9504410.